Triplet-odd pairing in finite nuclear systems: Even-even singly closed nuclei

Nobuo Hinohara,[1,2,3,*] Tomohiro Oishi,[4,5,†] and Kenichi Yoshida[6,1,4,‡]

[1]*Center for Computational Sciences, University of Tsukuba, Tsukuba, Ibaraki 305-8577, Japan*
[2]*Faculty of Pure and Applied Sciences, University of Tsukuba, Tsukuba, Ibaraki 305-8571, Japan*
[3]*Facility for Rare Isotope Beams, Michigan State University, East Lansing, Michigan 48824, USA*
[4]*RIKEN Nishina Center for Accelerator-Based Science, Wako, Saitama 351-0198, Japan*
[5]*Yukawa Institute for Theoretical Physics, Kyoto University, Kyoto 606-8502, Japan*
[6]*Research Center for Nuclear Physics, Osaka University, Ibaraki, Osaka 567-0047, Japan*

(Received 16 August 2023; revised 15 December 2023; accepted 22 January 2024; published 5 March 2024)

Background: The appearance of the pairing condensate is an essential feature of many-fermion systems. There are two possible types of pairing: spin-singlet and spin-triplet. However, an open question remains as to whether the spin-triplet pairing condensate emerges in finite nuclei.
Purpose: The aim of this work is to examine the coexistence of the spin-singlet and spin-triplet like-particle pairing condensates in nuclei. We also discuss the dependence on the type of pairing functional.
Method: The Hartree-Fock-Bogoliubov calculations with a Skyrme + local-pair energy-density functional (EDF) are performed to investigate the pairing condensate in the spherical ground states of Ca and Sn isotopes.
Results: The spin-singlet pair EDF induces not only the spin-singlet but also the spin-triplet pairing condensates due to a strong spin-orbit splitting. By discarding the spin-orbit EDF, only the spin-singlet pairing condensate appears. The spin-triplet pair EDF, however, induces the spin-orbit splitting and accordingly the spin-singlet pairing condensate.
Conclusions: The spin-orbit splitting plays an essential role in the coexistence of the spin-singlet and spin-triplet pairing condensates in nuclei.

DOI: 10.1103/PhysRevC.109.034302

I. INTRODUCTION

The pairing is universal in many-fermion systems [1,2]. A mean-field model was first introduced by Bardeen, Cooper, and Schrieffer (BCS) for describing the electronic superconductivity [3]. Within the original BCS theory, assumed is the condensation of a Cooper pair with a relative angular momentum being s wave, the total spin zero, and the center-of-mass momentum zero. A variety of forms of pairing, unconventional pairings, that are different from the BCS type have been also found or predicted; see the reviews [4–7] and the references therein. Especially, in electronic and cold-atomic systems, the spin-triplet Cooper pair has been actively investigated. The first example is the superfluidity of helium-3 atoms [8–10], where the spin-fluctuation interaction induces the spin-triplet Cooper pairs of fermionic atoms. The Fulde-Ferrell-Larkin-Ovchinnikov type of superconductivity, where the center-of-mass momentum is not zero, has been also discussed for decades [11–15]. In several spices of heavy-fermion metals and ferromagnetic Mott insulators [16–20], the spin-triplet type of superconductivity is expected. It is worthwhile to mention that spin-triplet pairing is a basic concept of topological superconductivity. For the emergence of spin-triplet pairing, the spin-orbit interaction often plays an essential role [4,6,21–23].

The pair correlation by a nucleon Cooper pair contributes significantly to low-energy nuclear physics. The BCS theory was applied to atomic nuclei soon after the original work [3] by Bohr *et al.* [24,25]. The like-particle spin-singlet pairing has been investigated mostly and is a key to understanding the low-energy properties of the nuclear structure, for example, the odd-even staggering (OES) of nuclear masses, the collectivity of the low-lying $J^\pi = 2^+$ states in even-even nuclei, and the moments of inertia of deformed nuclei [26,27]. The unconventional pairings have also been studied in nuclear systems. Since a deuteron is the only two-nucleon system that is bound in nature, the spin-triplet proton-neutron pairing has been investigated for a long time and is under lively discussions [7]. Similarly, due to the attractive nature of the nuclear force in the $^3P_2$ channel at high momentum, the emergence of the triplet-odd pairing has been predicted and studied in neutron-star matter [28–30].

For the study of nuclear superfluidity in medium-mass and heavy nuclei, a self-consistent mean-field or energy-density functional (EDF) approach has been adopted [31]. This choice is advantageous as it naturally provides the anomalous (pair) density and the pairing gap as an order parameter and the medium effects, which are known to be strong [1,32], can be captured in the EDF. Since the proton-neutron spin-triplet

*hinohara@nucl.ph.tsukuba.ac.jp
†tomohiro.oishi@ribf.riken.jp
‡kyoshida@rcnp.osaka-u.ac.jp

 ©2024 American Physical Society

pairing, as well as the isovector spin-singlet ones, can be characterized by local pair densities, there have been many studies for these types of pairing [33]. On the other side, discussions on the triplet-odd pairing in nuclei have been less active. In Refs. [34,35], the connection between the magnetic-dipole excitation to the triplet-odd pairing is suggested. However, experimental evidence of the triplet-odd pairing has not been observed.

In this work, we study the like-particle spin-triplet superfluidity in an EDF approach. To this end, we introduce the spin-triplet nonlocal pair density as an order parameter. We also investigate the connection between spin-orbit splitting and triplet-odd pairing.

II. FORMALISM

We describe the spin-singlet and spin-triplet pairing within the local density approximation of the EDF. Details on this framework are well summarized in Refs. [31,36,37], and in particular, we focus on the pairing part in this section.

A. Nonlocal pair density

The building block of the pairing in the Hartree-Fock-Bogoliubov (HFB) theory is the pair density matrix. We define it with the standard phase for the case without the proton-neutron pairing as

$$\hat{\tilde{\rho}}(\boldsymbol{r}_1 s_1, \boldsymbol{r}_2 s_2; t) = -2 s_2 \langle \Psi | \hat{c}_{\boldsymbol{r}_2 - s_2 t} \hat{c}_{\boldsymbol{r}_1 s_1 t} | \Psi \rangle, \tag{1}$$

where $\hat{c}_{\boldsymbol{r}st}$ represents the nucleon annihilation operator at position $\boldsymbol{r}$, spin s, and isospin t, and $|\Psi\rangle$ is the HFB state.

The spin-singlet and spin-triplet nonlocal pair densities are defined by

$$\tilde{\rho}_t(\boldsymbol{r}_1, \boldsymbol{r}_2) = \sum_s \hat{\tilde{\rho}}(\boldsymbol{r}_1 s, \boldsymbol{r}_2 s; t), \tag{2}$$

$$\tilde{\boldsymbol{s}}_t(\boldsymbol{r}_1, \boldsymbol{r}_2) = \sum_{s_1 s_2} \hat{\tilde{\rho}}(\boldsymbol{r}_1 s_1, \boldsymbol{r}_2 s_2; t) \hat{\boldsymbol{\sigma}}_{s_2 s_1}. \tag{3}$$

One can express the pair density matrix as

$$\hat{\tilde{\rho}}(\boldsymbol{r}_1 s_1, \boldsymbol{r}_2 s_2; t) = \tfrac{1}{2}\tilde{\rho}_t(\boldsymbol{r}_1, \boldsymbol{r}_2)\delta_{s_1 s_2} + \tfrac{1}{2}\tilde{\boldsymbol{s}}_t(\boldsymbol{r}_1, \boldsymbol{r}_2) \cdot \hat{\boldsymbol{\sigma}}_{s_1 s_2}, \tag{4}$$

where $\hat{\boldsymbol{\sigma}}$ is the spin Pauli matrix. We note that the nonlocal pair densities show the spatial property of the nucleon pair; the spin-singlet pair is symmetric and the spin-triplet pair is antisymmetric for the exchange of the coordinate variables,

$$\tilde{\rho}_t(\boldsymbol{r}_1, \boldsymbol{r}_2) = \tilde{\rho}_t(\boldsymbol{r}_2, \boldsymbol{r}_1), \tag{5}$$

$$\tilde{\boldsymbol{s}}_t(\boldsymbol{r}_1, \boldsymbol{r}_2) = -\tilde{\boldsymbol{s}}_t(\boldsymbol{r}_2, \boldsymbol{r}_1). \tag{6}$$

The spin-triplet nonlocal pair density vanishes at $\boldsymbol{r}_1 = \boldsymbol{r}_2$, indicating that a simple local density approximation does not work for the spin-triplet pair, and the nonlocality plays a major role here.

B. Density matrix expansion

The nuclear interaction energy derived from a local two-body interaction can be expressed with the local densities by a density matrix expansion technique. This has been discussed in Ref. [31] for the particle-hole part of the interaction. Here we apply the density matrix expansion for the pair density matrix (nonlocal pair density).

We introduce the following coordinates of the pair:

$$\boldsymbol{r}_1 = \boldsymbol{r} + \frac{\boldsymbol{r}_{\rm rel}}{2}, \quad \boldsymbol{r}_2 = \boldsymbol{r} - \frac{\boldsymbol{r}_{\rm rel}}{2}, \tag{7}$$

assuming that the pair density matrix vanishes quickly with increasing $\boldsymbol{r}_{\rm rel}$. This allows us to expand the nonlocal pair densities in terms of the relative coordinate $\boldsymbol{r}_{\rm rel}$:

$$\begin{aligned}
\tilde{\rho}_t(\boldsymbol{r}_1, \boldsymbol{r}_2) &= \tilde{\rho}_t\left(\boldsymbol{r} + \frac{\boldsymbol{r}_{\rm rel}}{2}, \boldsymbol{r} - \frac{\boldsymbol{r}_{\rm rel}}{2}\right) \\
&= \tilde{\rho}_t(\boldsymbol{r}, \boldsymbol{r}) + \frac{\partial}{\partial \boldsymbol{r}_{\rm rel}} \tilde{\rho}_t\left(\boldsymbol{r} + \frac{\boldsymbol{r}_{\rm rel}}{2}, \boldsymbol{r} - \frac{\boldsymbol{r}_{\rm rel}}{2}\right)\bigg|_{\boldsymbol{r}_{\rm rel}=\boldsymbol{0}} \cdot \boldsymbol{r}_{\rm rel} \\
&\quad + \frac{1}{2}\frac{\partial^2}{\partial \boldsymbol{r}_{\rm rel}^2} \tilde{\rho}_t\left(\boldsymbol{r} + \frac{\boldsymbol{r}_{\rm rel}}{2}, \boldsymbol{r} - \frac{\boldsymbol{r}_{\rm rel}}{2}\right)\bigg|_{\boldsymbol{r}_{\rm rel}=\boldsymbol{0}} \boldsymbol{r}_{\rm rel}^2 \\
&\quad + \mathcal{O}(|\boldsymbol{r}_{\rm rel}|^3) \\
&= \tilde{\rho}_t(\boldsymbol{r}) + \frac{1}{2}(\nabla_1 - \nabla_2)\tilde{\rho}_t(\boldsymbol{r}_1, \boldsymbol{r}_2)\bigg|_{\boldsymbol{r}_1=\boldsymbol{r}_2=\boldsymbol{r}} \cdot \boldsymbol{r}_{\rm rel} \\
&\quad + \frac{1}{8}(\nabla_1 - \nabla_2)^2 \tilde{\rho}_t(\boldsymbol{r}_1, \boldsymbol{r}_2)\bigg|_{\boldsymbol{r}_1=\boldsymbol{r}_2=\boldsymbol{r}} \boldsymbol{r}_{\rm rel}^2 + \mathcal{O}(|\boldsymbol{r}_{\rm rel}|^3) \\
&= \tilde{\rho}_t(\boldsymbol{r}) + \frac{1}{8}[\Delta\tilde{\rho}_t(\boldsymbol{r}) - 4\tilde{\tau}_t(\boldsymbol{r})]\boldsymbol{r}_{\rm rel}^2 + \mathcal{O}(|\boldsymbol{r}_{\rm rel}|^3).
\end{aligned} \tag{8}$$

We use $\tilde{\rho}_t(\boldsymbol{r}_1, \boldsymbol{r}_2) = \tilde{\rho}_t(\boldsymbol{r}_2, \boldsymbol{r}_1)$ to remove the first-order term, and the local pair density and kinetic pair density are defined as

$$\tilde{\rho}_t(\boldsymbol{r}) = \tilde{\rho}_t(\boldsymbol{r}, \boldsymbol{r}), \tag{9}$$

$$\tilde{\tau}_t(\boldsymbol{r}) = (\nabla_1 \cdot \nabla_2)\tilde{\rho}_t(\boldsymbol{r}_1, \boldsymbol{r}_2)|_{\boldsymbol{r}_1=\boldsymbol{r}_2=\boldsymbol{r}}. \tag{10}$$

The spin-triplet nonlocal pair density is expanded as

$$\begin{aligned}
\tilde{\boldsymbol{s}}_t(\boldsymbol{r}_1, \boldsymbol{r}_2) &= \tilde{\boldsymbol{s}}_t\left(\boldsymbol{r} + \frac{\boldsymbol{r}_{\rm rel}}{2}, \boldsymbol{r} - \frac{\boldsymbol{r}_{\rm rel}}{2}\right) \\
&= \boldsymbol{r}_{\rm rel} \cdot \left[\frac{\partial}{\partial \boldsymbol{r}_{\rm rel}} \otimes \tilde{\boldsymbol{s}}_t\left(\boldsymbol{r} + \frac{\boldsymbol{r}_{\rm rel}}{2}, \boldsymbol{r} - \frac{\boldsymbol{r}_{\rm rel}}{2}\right)\right]_{\boldsymbol{r}_{\rm rel}=\boldsymbol{0}} \\
&\quad + \mathcal{O}(|\boldsymbol{r}_{\rm rel}|^2) \\
&= \frac{1}{2}\boldsymbol{r}_{\rm rel} \cdot [(\nabla_1 - \nabla_2) \otimes \tilde{\boldsymbol{s}}_t(\boldsymbol{r}_1, \boldsymbol{r}_2)]\bigg|_{\boldsymbol{r}_1=\boldsymbol{r}_2=\boldsymbol{r}} \\
&\quad + \mathcal{O}(|\boldsymbol{r}_{\rm rel}|^2) \\
&= i\boldsymbol{r}_{\rm rel} \cdot \tilde{\mathrm{J}}_t(\boldsymbol{r}) + \mathcal{O}(|\boldsymbol{r}_{\rm rel}|^2),
\end{aligned} \tag{11}$$

where

$$\tilde{\mathrm{J}}_t(\boldsymbol{r}) = \frac{1}{2i}(\nabla_1 - \nabla_2) \otimes \tilde{\boldsymbol{s}}_t(\boldsymbol{r}_1, \boldsymbol{r}_2)\bigg|_{\boldsymbol{r}_1=\boldsymbol{r}_2=\boldsymbol{r}} \tag{12}$$

is the tensor (spin-current) pair density, we use $\tilde{\boldsymbol{s}}_t(\boldsymbol{r}_1, \boldsymbol{r}_2) = -\tilde{\boldsymbol{s}}_t(\boldsymbol{r}_2, \boldsymbol{r}_1)$ to remove the zeroth-order term, and $\boldsymbol{v} \cdot (\boldsymbol{u} \otimes \boldsymbol{w}) \equiv (\boldsymbol{v} \cdot \boldsymbol{u})\boldsymbol{w}$. Spin-triplet anisotropic pairing in condensed-matter physics requires an odd wave-number $\boldsymbol{k}$ dependence, and the tensor pair density corresponds to the order parameters of the p-wave superfluidity that consists of nine components [4].

The density matrix expansion of the nonlocal pair density provides the local EDF starting from a local two-body spin-singlet and spin-triplet pairing interaction. The general form

of the pair EDF is given by [38]

$$E^{S=0}_{\text{pair},t} = \int d\boldsymbol{r}_1 d\boldsymbol{r}_2 v^{S=0}_{\text{pair},t}(|\boldsymbol{r}_1 - \boldsymbol{r}_2|)|\tilde{\rho}_t(\boldsymbol{r}_1,\boldsymbol{r}_2)|^2, \tag{13}$$

$$E^{S=1}_{\text{pair},t} = \int d\boldsymbol{r}_1 d\boldsymbol{r}_2 v^{S=1}_{\text{pair},t}(|\boldsymbol{r}_1 - \boldsymbol{r}_2|)|\tilde{\boldsymbol{s}}_t(\boldsymbol{r}_1,\boldsymbol{r}_2)|^2, \tag{14}$$

where $v^{S=0}_{\text{pair},t}$ and $v^{S=1}_{\text{pair},t}$ are the spin-singlet and spin-triplet pairing interaction strengths that depend on the absolute value of the relative coordinate of the two nucleons.

Inserting the density matrix expansion in the nonlocal pair densities, we have

$$E^{S=0}_{\text{pair},t} = \int d\boldsymbol{r}\big\{\tilde{C}^{\rho}_t|\tilde{\rho}_t(\boldsymbol{r})|^2 + \tilde{C}^{\Delta\rho}_t \text{Re}[\tilde{\rho}^*_t(\boldsymbol{r})\Delta\tilde{\rho}_t(\boldsymbol{r})] + \tilde{C}^{\tau}_t \text{Re}[\tilde{\rho}^*_t(\boldsymbol{r})\tilde{\tau}_t(\boldsymbol{r})]\big\}, \tag{15}$$

$$E^{S=1}_{\text{pair},t} = \int d\boldsymbol{r}\tilde{C}^{J}_t|\tilde{\mathsf{J}}_t(\boldsymbol{r})|^2. \tag{16}$$

The coupling constants are related to the local potential as

$$\tilde{C}^{\rho}_t = \int d\boldsymbol{r}_{\text{rel}} v^{S=0}_{\text{pair},t}(|\boldsymbol{r}_{\text{rel}}|), \tag{17}$$

$$\tilde{C}^{\Delta\rho}_t = -\frac{1}{4}\tilde{C}^{\tau}_t = \frac{1}{4}\int d\boldsymbol{r}_{\text{rel}}\boldsymbol{r}^2_{\text{rel}} v^{S=0}_{\text{pair},t}(|\boldsymbol{r}_{\text{rel}}|), \tag{18}$$

$$\tilde{C}^{J}_t = \int d\boldsymbol{r}_{\text{rel}}\boldsymbol{r}^2_{\text{rel}} v^{S=1}_{\text{pair},t}(|\boldsymbol{r}_{\text{rel}}|). \tag{19}$$

These are the coupling constants for the spin-singlet pairing $\tilde{C}^{\rho}_t$ and its next-order terms $\tilde{C}^{\Delta\rho}_t$ and $\tilde{C}^{\tau}_t$, and the spin-triplet coupling constant $\tilde{C}^{J}_t$.

By using the G3RS-^{1}E-1 potential introduced by Tamagaki [28], for instance, $\tilde{C}^{\rho}_t = -697.087$ MeV fm^3 and $\tilde{C}^{\Delta\rho}_t = 1363.253$ MeV fm^5 are obtained for the spin-singlet coupling constants. For the spin-triplet coupling, on the other hand, by using the G3RS-^{3}O-1 potential for $v^{S=1}_{\text{pair},t}$, we obtain $\tilde{C}^{J}_t = 6794.724$ MeV fm^5. Note that we assumed the $^3P_1$ channel to obtain this value and that this is repulsive in this channel.

In the lowest order in terms of the nonlocality, the local pair density $\tilde{\rho}_t(\boldsymbol{r})$ and the pair EDF that is proportional to $|\tilde{\rho}_t(\boldsymbol{r})|^2$ represent the spin-singlet pair condensation and EDF, while the spin-current pair density $\tilde{\mathsf{J}}_t(\boldsymbol{r})$ and the term proportional to $|\tilde{\mathsf{J}}_t(\boldsymbol{r})|^2$ represent the spin-triplet pair condensation and EDF.

Zero-range Skyrme interactions also produce the terms related to the spin-singlet and spin-triplet pair condensation. Only the SkP interaction [39] includes the spin-singlet and spin-triplet terms, and other standard Skyrme EDFs do not consider pairing terms other than those proportional to $|\tilde{\rho}_t(\boldsymbol{r})|^2$ due to unrealistic pairing properties [31].

We note that the spin-triplet pair density and thus the EDF can be decomposed into trace (pseudoscalar), antisymmetric (vector), and symmetric (pseudotensor) parts [37]:

$$\tilde{J}_t(\boldsymbol{r}) = \sum_{a=x,y,z}\tilde{\mathsf{J}}_{taa}(\boldsymbol{r}), \tag{20}$$

$$\tilde{\boldsymbol{J}}_{ta}(\boldsymbol{r}) = \sum_{b,c=x,y,z}\epsilon_{abc}\tilde{\mathsf{J}}_{tbc}(\boldsymbol{r}), \tag{21}$$

$$\underline{\tilde{\mathsf{J}}}_{tab}(\boldsymbol{r}) = \tfrac{1}{2}\tilde{\mathsf{J}}_{tab}(\boldsymbol{r}) + \tfrac{1}{2}\tilde{\mathsf{J}}_{tba}(\boldsymbol{r}) - \tfrac{1}{3}\tilde{J}_t(\boldsymbol{r})\delta_{ab}. \tag{22}$$

This decomposition of the spin-current quantity is also applied in the discussion of $^3P_2$ superfluidity [40,41], and these three components are relevant to $^3P_0$, $^3P_1$, and $^3P_2$ superfluidity, respectively.

For a general pair EDF that is not based on an effective interaction, each coupling constant in the spin-singlet pair EDF (15) can be taken independently, except that the relation between $\tilde{C}^{\Delta\rho}_t$ and $\tilde{C}^{\tau}_t$ in Eq. (18) is a requirement from the local gauge invariance [37]. The spin-triplet pair EDF has a structure similar to that of the tensor functional in the particle-hole EDF and can have a more general form [42]:

$$E^{S=1}_{\text{pair},t} = \int d\boldsymbol{r}\tilde{C}^{J0}_t|\tilde{J}_t(\boldsymbol{r})|^2 + \tilde{C}^{J1}_t|\tilde{\boldsymbol{J}}_t(\boldsymbol{r})|^2 + \tilde{C}^{J2}_t|\underline{\tilde{\mathsf{J}}}_t(\boldsymbol{r})|^2. \tag{23}$$

Unlike the particle-hole part, these three coupling constants are not constrained by the local gauge invariance and can be taken independently. When the pair EDF is derived from a nonlocal effective interaction of the form (14), three coupling constants are related by $\tilde{C}^{J}_t = 3\tilde{C}^{J0}_t = 2\tilde{C}^{J1}_t = \tilde{C}^{J2}_t$. However, the tensor and spin-orbit interactions, which are not in the form of Eq. (14), allow independent contributions to the three coupling constants.

C. Mean-field approach

The mean-field equations for protons and neutrons, obtained by the functional derivative of the EDF, are given in Refs. [37,39]. The pair Hamiltonian has the following form:

$$\tilde{h}^{(t)}_{ss'}(\boldsymbol{r}) = [\tilde{U}_t(\boldsymbol{r}) - \nabla\tilde{M}_t(\boldsymbol{r})\cdot\nabla]\delta_{ss'} + \frac{1}{2i}\{\nabla\cdot[\tilde{\mathsf{B}}_t(\boldsymbol{r})\cdot\hat{\boldsymbol{\sigma}}_{ss'}] + [\tilde{\mathsf{B}}_t(\boldsymbol{r})\cdot\hat{\boldsymbol{\sigma}}_{ss'}]\cdot\nabla\}, \tag{24}$$

where the potential energy $\tilde{U}_t$, the effective inertia parameter $\tilde{M}_t$, and the spin-orbit form factors $\tilde{\mathsf{B}}_t$ are given by

$$\tilde{U}_t(\boldsymbol{r}) = 2\tilde{C}^{\rho}_t\tilde{\rho}_t(\boldsymbol{r}) + 2\tilde{C}^{\Delta\rho}_t\Delta\tilde{\rho}_t(\boldsymbol{r}) + \tilde{C}^{\tau}_t\tilde{\tau}_t(\boldsymbol{r}), \tag{25}$$

$$\tilde{M}_t(\boldsymbol{r}) = \tilde{C}^{\tau}_t\tilde{\rho}_t(\boldsymbol{r}), \tag{26}$$

$$\tilde{\mathsf{B}}_{tab}(\boldsymbol{r}) = 2\tilde{C}^{J0}_t\tilde{J}_t(\boldsymbol{r})\delta_{ab} - 2\tilde{C}^{J1}_t\sum_{c=x,y,z}\epsilon_{acb}\tilde{\boldsymbol{J}}_{tc}(\boldsymbol{r}) + 2\tilde{C}^{J2}_t\underline{\tilde{\mathsf{J}}}_{tab}(\boldsymbol{r}). \tag{27}$$

As the pair Hamiltonian (24) depends on the spins s and s' when spin-triplet pair EDF is considered, we define the pairing gap by averaging out the pair Hamiltonian using the spin-dependent lower component of the quasiparticle wave function $\phi^{(t)}_2(\mu,\boldsymbol{r}s)$ as

$$\Delta_t = \frac{\int d\boldsymbol{r}\sum_{ss'\mu}\phi^{(t)*}_2(\mu,\boldsymbol{r}s')\tilde{h}^{(t)}_{s's}(\boldsymbol{r})\phi^{(t)}_2(\mu,\boldsymbol{r}s)}{\int d\boldsymbol{r}\sum_{s\mu}|\phi^{(t)}_2(\mu,\boldsymbol{r}s)|^2} = \frac{1}{N_t}\int d\boldsymbol{r}[\tilde{U}_t(\boldsymbol{r})\rho_t(\boldsymbol{r}) + \tilde{M}_t(\boldsymbol{r})\tau_t(\boldsymbol{r}) + \tilde{\mathsf{B}}_t(\boldsymbol{r})\cdot\mathsf{J}_t(\boldsymbol{r})], \tag{28}$$

where $N_t = N$ or Z, and the density ρ_t, the kinetic density τ_t, and the tensor (spin-current) density J_t are defined using the

nonlocal particle-hole densities [defined in a similar way as Eqs. (2) and (3) but for the particle-hole density matrix] as

$$\rho_t(\boldsymbol{r}) = \rho_t(\boldsymbol{r},\boldsymbol{r}), \tag{29}$$

$$\tau_t(\boldsymbol{r}) = (\nabla_1\cdot\nabla_2)\rho_t(\boldsymbol{r}_1,\boldsymbol{r}_2)|_{\boldsymbol{r}_1=\boldsymbol{r}_2=\boldsymbol{r}}, \tag{30}$$

$$\mathrm{J}_t(\boldsymbol{r}) = \frac{1}{2i}(\nabla_1-\nabla_2)\otimes\boldsymbol{s}_t(\boldsymbol{r}_1,\boldsymbol{r}_2)\Big|_{\boldsymbol{r}_1=\boldsymbol{r}_2=\boldsymbol{r}}. \tag{31}$$

Although Eq. (28) is a natural extension of the average gap for a generalized pair Hamiltonian [43], the discrepancy of the pairing gap and experimental OES has been pointed out when the singlet-pair EDF contains the kinetic terms $\tilde{C}_t^{\tau}$ and $\tilde{C}_t^{\Delta\rho}$ [44].

D. Expression within spherical symmetry

We assume the spherical symmetry for the HFB state for simplicity. The spherical symmetry cancels the two of the spin-current pair densities $\tilde{\boldsymbol{J}}_t(\boldsymbol{r})$ and $\tilde{\mathrm{J}}_t(\boldsymbol{r})$, and only the radial component of the vector spin-current pair density can exist, $\tilde{\boldsymbol{J}}_t(\boldsymbol{r}) = \tilde{J}_{tr}(r)\boldsymbol{e}_r$ [45]. Within the spherical symmetry, the quasiparticle wave function can be decomposed into the radial and angular part:

$$\phi_i^{(t)}(E,\boldsymbol{r}s) = \frac{u_i^{(t)}(nlj,r)}{r}Y_{lm_l}(\hat{\boldsymbol{r}})\left\langle lm_l\frac{1}{2}s|jm\right\rangle \quad (i=1,2), \tag{32}$$

where $i=1$ and 2 correspond to the upper and lower components, respectively. The local pair density and the spin-current pair density are given by

$$\tilde{\rho}_t(r) = -\frac{1}{4\pi r^2}\sum_{nlj}(2j+1)u_1^{(t)}(nlj,r)u_2^{(t)}(nlj,r), \tag{33}$$

$$\tilde{J}_{tr}(r) = -\frac{2}{4\pi r^3}\sum_{nlj}(2j+1)\langle\boldsymbol{l}\cdot\boldsymbol{s}\rangle u_1^{(t)}(nlj,r)u_2^{(t)}(nlj,r), \tag{34}$$

where $\langle\boldsymbol{l}\cdot\boldsymbol{s}\rangle = \frac{1}{2}[j(j+1)-l(l+1)-\frac{3}{4}]$. Notice that these quantities have different dimensions.

III. NUMERICAL CALCULATIONS

A. Spin-singlet pair EDF

We utilize the HFBRAD code [46] for spherical Skyrme-HFB calculations in the following. The SLy4 and spin-singlet volume-type contact pair EDF with the strength $\tilde{C}_n^{\rho} = -46.625$ MeV fm^3 (in the standard notation $V_0 = 4\tilde{C}_n^{\rho} = -186.5$ MeV fm^3) is employed with the cutoff parameter of 60 MeV. This strength has been adjusted to reproduce the neutron pairing gap 1.245 MeV in ^{120}Sn.

We evaluate the spin-singlet and spin-triplet pair condensations with the following pairing components:

$$S_{\rho_n} = \int d\boldsymbol{r}|\tilde{\rho}_t(\boldsymbol{r})|^2, \tag{35}$$

$$S_{J_n} = R^2\int d\boldsymbol{r}|\tilde{\boldsymbol{J}}_t(\boldsymbol{r})|^2. \tag{36}$$

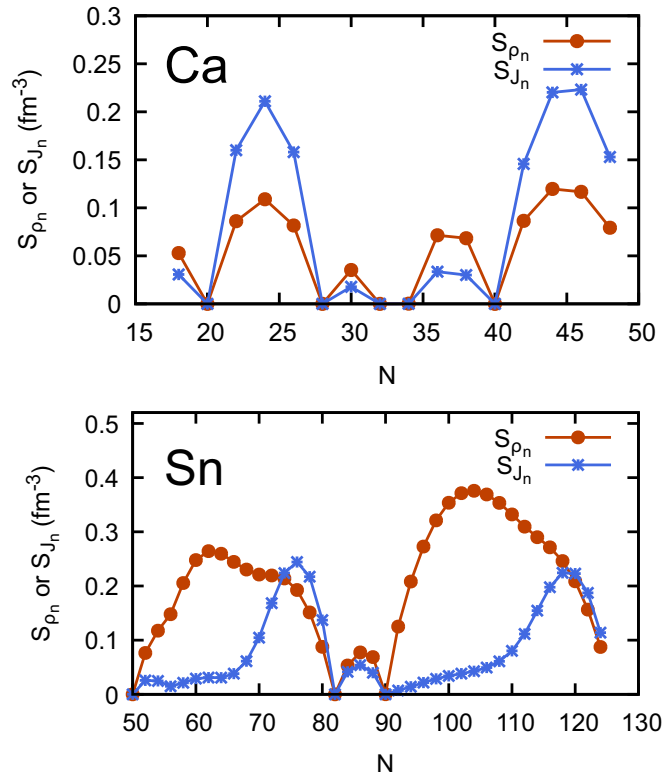

FIG. 1. Spin-singlet and triplet pairing components of neutrons, S_{ρ_n} and S_{J_n}, respectively, in the Ca and Sn isotope chains.

They have exactly the same local density dependence that appears in the pair energy. The constant $R^2 = 10$ fm^2 is estimated from the ratio $|\tilde{C}_t^J/\tilde{C}_t^{\rho}|$ of the G3RS potential and is introduced to make the units of the two quantities identical.

In Fig. 1, the results from neutron pair densities in the Ca and Sn isotopes are presented. The spin-singlet component S_{ρ_n} shows finite values except in neutron closed-shell nuclei. Even though the attractive pair EDF is present only in the spin-singlet channel, our results show nonzero values for the spin-triplet component S_{J_n}, namely, a coexistence of the spin-singlet and spin-triplet condensates is suggested in finite nuclei. This is also expected in Eqs. (33) and (34). A similar feature has been discussed in condensed matter [21] and ultracold Fermi gas [22,23,47] in the presence of the spin-orbit ($\boldsymbol{k}\otimes\boldsymbol{\sigma}$ type) interaction. Notice that a direct comparison of S_{ρ_n} and S_{J_n} does not make sense as their relative value depends on the introduced constant R^2. However, the isotopic dependence indicates that the spin-triplet pairing is more sensitive to the shell orbits involved than the spin-singlet one is. S_{ρ_n} is enhanced in the midshell region with high degeneracy, such as in the $f_{7/2}$ and $f_{5/2}$ orbits in Ca isotopes and $50 < N < 82$ and $82 < N < 126$ in Sn isotopes, while S_{J_n} shows a stronger orbital dependence; we see an enhancement (a reduction) in S_{J_n} in the isotope where the neutron Fermi energy is around $j_>$ ($j_<$) orbit in $f_{7/2}$ and $f_{5/2}$ in Ca isotopes and an enhancement in the intruder region in the middle shell in Sn isotopes.

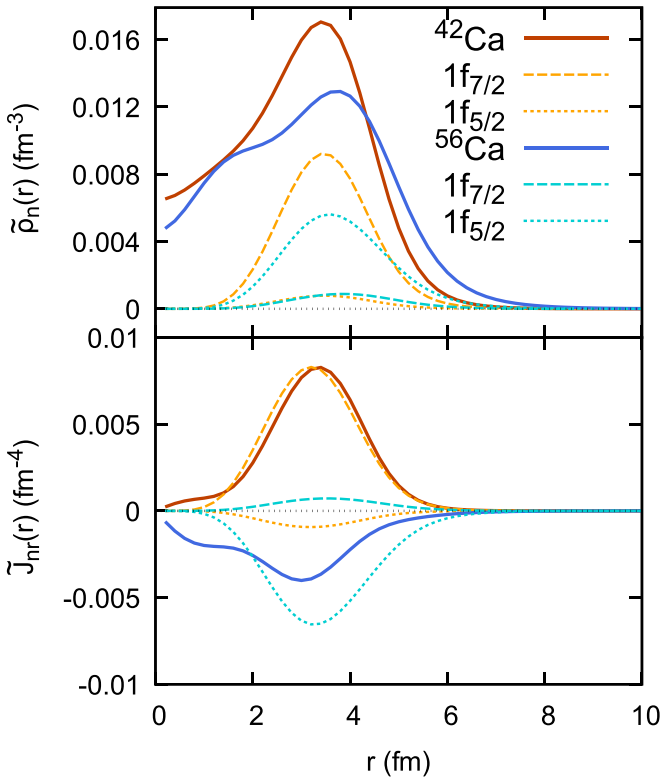

FIG. 2. The neutron local pair density $\tilde{\rho}_n(r)$ and the radial component of the neutron tensor pair density $\tilde{J}_{nr}(r)$ of ^{42}Ca and ^{56}Ca and the contributions from $1f_{7/2}$ and $1f_{5/2}$ orbits.

To analyze the contributions from the $j_>$ and $j_<$ orbits, we take ^{42}Ca and ^{56}Ca as representative cases, where two particles are supposed to occupy the $f_{7/2}$ and $f_{5/2}$ orbits mainly. The pair density distributions $\tilde{\rho}_n(r)$ and $\tilde{J}_{nr}(r)$ together with the contributions from $f_{7/2}$ and $f_{5/2}$ orbits are plotted in Fig. 2. Both the spin-singlet and spin-triplet neutron pair densities have finite values in the ^{42}Ca and ^{56}Ca nuclei. There, the $f_{7/2}$ and $f_{5/2}$ neutrons have dominant contributions as expected. For the spin-singlet density, they have a coherent contribution, and the total pair densities are composed of the coherent addition from the other orbits as well (not shown in the figure), whereas the neutrons in the $f_{7/2}$ and $f_{5/2}$ orbits contribute in a destructive way to the spin-triplet density. The dominant contribution for $\tilde{J}_{nr}(r)$ in ^{42}Ca is from the $f_{7/2}$ orbit, while $\tilde{J}_{nr}(r)$ in ^{56}Ca is composed of the multiple orbits including those not shown in the figure. This indicates the magicity at $N = 34$ is weaker than that at $N = 28$.

B. Spin-triplet pair EDF

In place of the spin-singlet pair EDF, we employ the spin-triplet pair EDF. The coupling constant of the spin-triplet pair EDF is adjusted to reproduce the pairing energy of ^{44}Ca obtained in the spin-singlet pair EDF ($\tilde{C}_n^{J1} = -46.125$ MeV fm^5). The pairing energy is -5.08 and -5.25 MeV in the singlet-pair EDF and triplet-pair EDF, as shown in Figs. 4(c) and 4(d).

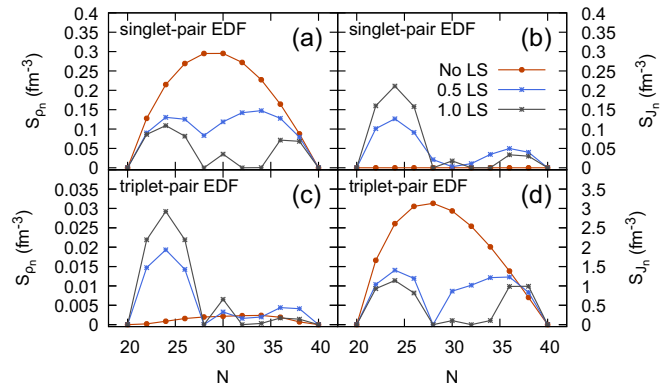

FIG. 3. Spin-singlet and spin-triplet pairing components, S_{ρ_n} and S_{J_n}, calculated in the Ca isotopes by changing the coupling constant of the spin-orbit EDF. The labels 1.0 LS, 0.5 LS, and no LS represent the calculations with the original spin-orbit EDF, the reduced one multiplied by a factor of 0.5, and the calculation without the spin-orbit EDF, respectively.

Figure 3 shows the spin-singlet and spin-triplet pairing components calculated with either the spin-singlet or the spin-triplet pair EDF for the Ca isotopes. The spin-singlet pairing component calculated with the spin-singlet pair EDF and the spin-triplet pairing component calculated with the spin-triplet pair EDF have very similar properties: one sees the collapse of the pairing at the magic numbers $N = 20$, 28, 32, and 40 (there is a tiny difference in $N = 34$) and the neutron-number dependence of the relative size of the pairing component. We also note that there is little difference in the pairing energy, the chemical potential, and other observables of the particle-hole type. The coupling constant of the spin-triplet pair EDF $\tilde{C}_t^{J1}$ can be related to the Skyrme parameters as $\tilde{C}_t^{J1} = [t_2(1 + x_2) + 5t_o + 2W_0)]/8$ and are repulsive for many Skyrme interactions such as SIII (18.125 MeV fm^5) [48], SLy4 (30.75 MeV fm^5), SLy5 (31.5 MeV fm^5) [49], and SkP (5.486 MeV fm^5), but can be attractive for the Skyrme interactions that include the tensor interaction such as SLy5 + T (-53.5 MeV fm^5) [50], and 14 Skyrme parameters out

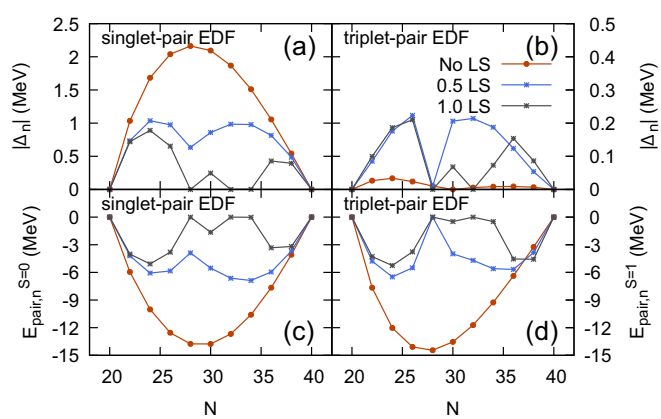

FIG. 4. Pairing gap $|\Delta_n|$ and pairing energy $E_{\mathrm{pair},n}^{S=0,1}$ calculated for the singlet- and triplet-pair EDFs in the Ca isotopes by changing the coupling constant of the spin-orbit EDF.

of 36 T*IJ* parameter sets in Ref. [51]. Although the coupling constants of the EDF can be taken arbitrarily in the framework of the nuclear density functional theory, the tensor interaction will have a large impact on the property of the spin-triplet pairing coupling constant.

C. Roles of the spin-orbit EDF

The spin-orbit splitting is expected to play an important role in the spin-triplet pairing as anticipated from the expression of the tensor pair density (34). In Fig. 3, we also present the pairing components S_{ρ_n} and S_{J_n} obtained by changing the coupling constant of the spin-orbit EDF while keeping the pairing coupling constants to the original values. Three spin-orbit EDFs are considered: the original spin-orbit EDF (1.0 LS), the reduced one multiplied by a factor of 0.5 (0.5 LS), and no spin-orbit EDF (No LS). First, suppose that the spin-orbit EDF is neglected. Then, the spin-singlet pair EDF promotes only the spin-singlet pair condensate, and the spin-triplet pairing component S_{J_n} is zero [Figs. 3(a) and 3(b)]. One is tempted to the opposite conclusion when the spin-triplet pair EDF is considered. However, the appearance of the spin-triplet pairing component inevitably induces the spin-orbit splitting and the spin-singlet pairing component. This results in a nonzero spin-singlet pairing component, although the induced amount is tiny. As a result, commonly with the spin-singlet and spin-triplet EDFs, the corresponding pairing component takes the maximum at around $N = 28$, which is around the half-filled situation of the 14-fold degenerated f orbit [Figs. 3(a) and 3(d)]. The pairing component becomes zero at LS-closed shells $N = 20$ and $N = 40$.

The behavior of the pairing components S_{ρ_n} and S_{J_n} shows a drastic change with the value of the coupling constant of the spin-orbit EDF, although we do not change the pair EDF itself. The spin-orbit EDF decreases the pairing component due to the lower degeneracy of the single-particle levels [Figs. 3(a) and 3(d)], but it enhances the coexistence of S_{ρ_n} and S_{J_n} [Figs. 3(b) and 3(c)].[1] By comparing the 0.5 LS and 1.0 LS cases, one can see an enhancement of the mixing in the region $20 < N < 28$ and the suppression in the neutron-rich side with $N > 30$. The suppression is common for the main pairing component and the induced pairing component due to the lesser degeneracy of the single-particle levels with increasing the coupling constant of the spin-orbit EDF.

We also plot the pairing gap and the pairing energy in Fig. 4. Figures 3(a) and 4(a) show that the singlet-pairing component S_{ρ_n} and the pairing gap Δ_n behave in a similar way in the case of singlet-pair EDF, while the triplet-pairing component S_{J_n} [Fig. 3(d)] and the pairing gap [Fig. 4(b)] in the case of the triplet-pair EDF behave in a different way. A strong reduction of the averaged gap for the triplet pairing in the "No LS" case [Fig. 4(b)] is due to a low tensor density J. The pairing energies for the singlet-pair EDF [Fig. 4(c)] and the triplet-pair EDF [Fig. 4(d)] take similar values as a function of the neutron number, although the coupling constants of the two pair EDFs are adjusted only at $N = 24$. The agreement of the pairing energy shows that the triplet-pair EDF can include a contribution similar to that of the singlet-pair EDF.

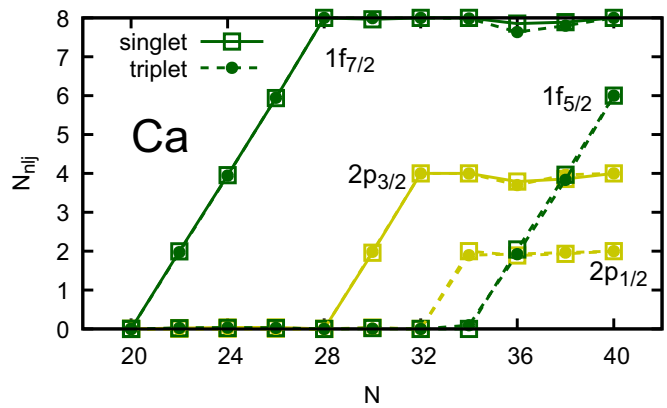

FIG. 5. Occupation numbers of pf-shell orbits in Ca isotopes calculated with the singlet- and triplet-pair EDFs.

D. Relevant observables

The small values of the pairing gap defined by Eq. (28) may not correspond to the experimental OES for the triplet-pair EDF [Fig. 4(b)], similar to when the singlet-pair Hamiltonian contains derivative terms [44]. We note that another average gap in which $\phi_2^{(t)*}$ is replaced by $\phi_1^{(t)*}$ in Eq. (28) behaves even worse in the case of the triplet-pair EDF, because of the singlet-pair amplitude in the denominator that is very small as expected from Fig. 3(c).

To analyze the influence of the type of pairing in the occupation, we plot the occupation of each neutron orbit in Fig. 5. The occupation number increases in the order of the single-particle energies with the neutron number increases, showing that the dominant pair correlation is within a single orbit near the Fermi energy. There is no significant difference between the occupation numbers calculated with the singlet- and triplet-pair EDFs. The difference is barely visible around $34 \leqslant N \leqslant 38$.

The pairing rotational moment of inertia can be a relevant observable of the pairing condensation [53] even in the presence of the triplet-pair EDF. Figure 6 shows the two-neutron separation energies $S_{2n}(N) = E(N-2) - E(N)$ and the neutron pairing rotational moments of inertia calculated from the three HFB energy differences $\mathcal{J}_n(N) = 4/\Delta S_{2n}(N) = 4/[E(N+2) - 2E(N) + E(N-2)]$. Unlike the relation between the pairing gap and the OES, the pairing rotational moment of inertia holds a good correspondence with the experimental values of the double binding-energy differences. The moment of inertia at $N = 30$ becomes negative (-17.86 MeV^{-1}) for the triplet-pair EDF, while the singlet-pair EDF reproduces the experimental value. The negative value originates from the staggering behavior of S_{2n} at $N = 30$ seen in Fig. 6(a). Two of the HFB states ($N = 28$ and 32) used to computed the inertia at $N = 30$ are in the normal

[1]The mixture of the spin-singlet (even-parity) and spin-triplet (odd-parity) components due to the spin-orbit field was discussed in the proton-neutron channel within the three-body model for ^{16}O$+p+n$ [52].

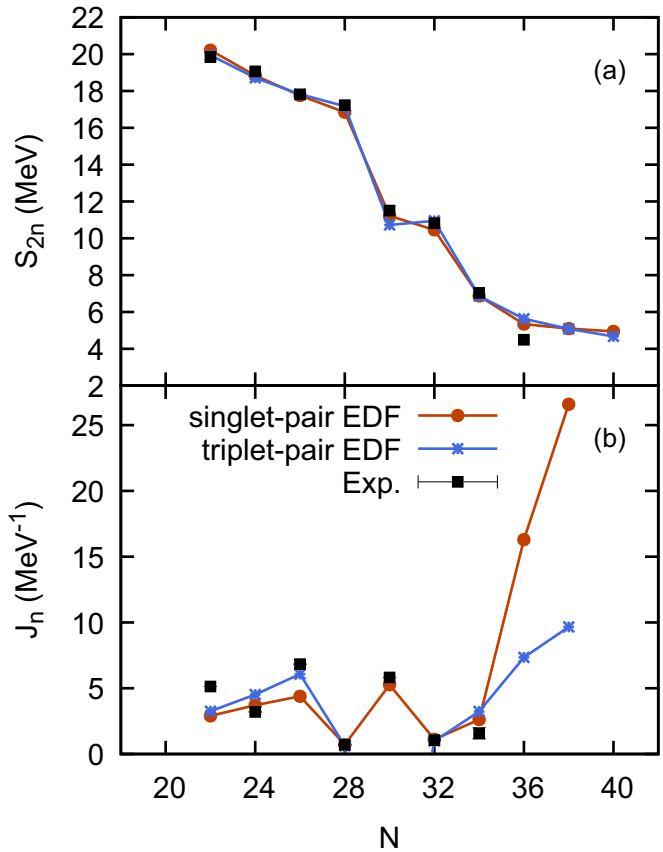

FIG. 6. Two-neutron separation energies and moments of inertia of the neutron pairing rotation in the Ca isotopes calculated for the singlet- and triplet-pair EDFs. The inertia calculated with the triplet-pair EDF at $N = 30$ (-17.86 MeV^{-1}) is not shown in the figure.

states corresponding to the $f_{7/2}$ and $p_{3/2}$ shell closures, and the inertia at $N = 30$ does not correspond to the pairing indicator, as the expression of the inertia based on the double binding-energy differences assumes that the three nearby isotopes have similar pairing structures, and this assumption does not hold in this case. We can see a difference in the moment of inertia in the neutron-rich region at $N = 36$ and 38 for the singlet-pair and triplet-pair EDFs. The binding energies in the neutron-rich isotopes may determine the coupling constant of the triplet-pair EDF.

IV. SUMMARY

We analyzed the spin-triplet pair condensation of like particles in singly closed nuclei. The relevant quantity to the spin-triplet pair condensation is the nine-component spin-current pair density. One component can be finite in the HFB calculation within the spherical symmetry. We have demonstrated that the spin-singlet and spin-triplet pairing condensates coexist in open-shell nuclei, and one component of the pair EDF can induce the other component. The spin-orbit splitting is shown to play an essential role in the coexistence of the two types of pair condensates, because the spin is no longer a good quantum number.

The inclusion of both the spin-singlet and spin-triplet pair EDFs into the nuclear EDF will enable us more detailed description of the nuclear pairing condensation, including the isotope and isotone dependence, and deepen the understanding of the origin of the spin-orbit splitting and the role of the tensor force in the pairing channel. In describing open-shell nuclei with deformation, the pseudoscalar and pseudotensor components should be considered. In subsequent works, we will present such developments.

ACKNOWLEDGMENTS

The authors express their sincere gratitude to T. Naito, W. Nazarewicz, H. Tajima, and Y. Yanase for their conscientious review of the manuscript and invaluable insights. Additionally, the authors acknowledge the invaluable contributions of members of the PHANES Collaboration (M. Dozono, M. Matsuo, S. Ota, and S. Shimoura) for their insightful discussions. This work was supported by the JSPS KAKENHI (Grants No. JP19K03824, No. JP19K03872, No. JP19KK0343, and No. JP20K03964).

[1] D. J. Dean and M. Hjorth-Jensen, Pairing in nuclear systems: from neutron stars to finite nuclei, Rev. Mod. Phys. **75**, 607 (2003).
[2] D. M. Brink and R. A. Broglia, *Nuclear Superfluidity: Pairing in Finite Systems*, Cambridge Monographs on Particle Physics, Nuclear Physics and Cosmology (Cambridge University, Cambridge, England, 2005).
[3] J. Bardeen, L. N. Cooper, and J. R. Schrieffer, Theory of superconductivity, Phys. Rev. **108**, 1175 (1957).
[4] M. Sigrist and K. Ueda, Phenomenological theory of unconventional superconductivity, Rev. Mod. Phys. **63**, 239 (1991).
[5] T. Takatsuka and R. Tamagaki, Superfluidity in neutron star matter and symmetric nuclear matter, Prog. Theor. Phys. Suppl. **112**, 27 (1993).
[6] A. P. Mackenzie and Y. Maeno, The superconductivity of Sr_2RuO_4 and the physics of spin-triplet pairing, Rev. Mod. Phys. **75**, 657 (2003).
[7] S. Frauendorf and A. O. Macchiavelli, Overview of neutron–proton pairing, Prog. Part. Nucl. Phys. **78**, 24 (2014).
[8] D. D. Osheroff, R. C. Richardson, and D. M. Lee, Evidence for a new phase of solid He^3, Phys. Rev. Lett. **28**, 885 (1972).
[9] D. D. Osheroff, W. J. Gully, R. C. Richardson, and D. M. Lee, New magnetic phenomena in liquid He^3 below 3 mK, Phys. Rev. Lett. **29**, 920 (1972).
[10] A. J. Leggett, Interpretation of recent results on He^3 below 3 mK: A new liquid phase? Phys. Rev. Lett. **29**, 1227 (1972).
[11] P. Fulde and R. A. Ferrell, Superconductivity in a strong spin-exchange field, Phys. Rev. **135**, A550 (1964).

[12] A. I. Larkin and Y. N. Ovchinnikov, Nonuniform state of superconductors, Zh. Eksp. Teor. Fiz. **47**, 1136 (1964).

[13] R. Casalbuoni and G. Nardulli, Inhomogeneous superconductivity in condensed matter and QCD, Rev. Mod. Phys. **76**, 263 (2004).

[14] Y. Yanase, Angular Fulde-Ferrell-Larkin-Ovchinnikov state in cold fermion gases in a toroidal trap, Phys. Rev. B **80**, 220510(R) (2009).

[15] F. S. Bergeret and A. F. Volkov, Triplet odd-frequency superconductivity in hybrid superconductor–ferromagnet structures, Ann. Phys. **456**, 169232 (2023).

[16] D. Aoki, K. Ishida, and J. Flouquet, Review of U-based ferromagnetic superconductors: Comparison between UGe_2, URhGe, and UCoGe, J. Phys. Soc. Jpn. **88**, 022001 (2019).

[17] W. Cai, H. Sun, W. Xia, C. Wu, Y. Liu, H. Liu, Y. Gong, D.-X. Yao, Y. Guo, and M. Wang, Pressure-induced superconductivity and structural transition in ferromagnetic $CrSiTe_3$, Phys. Rev. B **102**, 144525 (2020).

[18] S. Ran, C. Eckberg, Q.-P. Ding, Y. Furukawa, T. Metz, S. R. Saha, I.-L. Liu, M. Zic, H. Kim, J. Paglione, and N. P. Butch, Nearly ferromagnetic spin-triplet superconductivity, Science **365**, 684 (2019).

[19] L. Jiao, S. Howard, S. Ran, Z. Wang, J. O. Rodriguez, M. Sigrist, Z. Wang, N. P. Butch, and V. Madhavan, Chiral superconductivity in heavy-fermion metal UTe_2, Nature (London) **579**, 523 (2020).

[20] E. J. König, Y. Komijani, and P. Coleman, Triplet resonating valence bond theory and transition metal chalcogenides, Phys. Rev. B **105**, 075142 (2022).

[21] L. P. Gor'kov and E. I. Rashba, Superconducting 2D system with lifted spin degeneracy: Mixed singlet-triplet state, Phys. Rev. Lett. **87**, 037004 (2001).

[22] H. Hu, L. Jiang, X.-J. Liu, and H. Pu, Probing anisotropic superfluidity in atomic Fermi gases with Rashba spin-orbit coupling, Phys. Rev. Lett. **107**, 195304 (2011).

[23] J. P. Vyasanakere, S. Zhang, and V. B. Shenoy, BCS-BEC crossover induced by a synthetic non-Abelian gauge field, Phys. Rev. B **84**, 014512 (2011).

[24] A. Bohr, B. R. Mottelson, and D. Pines, Possible analogy between the excitation spectra of nuclei and those of the superconducting metallic state, Phys. Rev. **110**, 936 (1958).

[25] A. Bohr and B. R. Mottelson, *Nuclear Structure* (Benjamin, New York, 1969).

[26] P. Ring and P. Schuck, *The Nuclear Many-Body Problems*, Texts and Monographs in Physics (Springer-Verlag, New York, 1980).

[27] *Fifty Years of Nuclear BCS: Pairing in Finite Systems*, edited by R. A. Broglia and V. Zelevinsky (World Scientific, Singapore, 2013).

[28] R. Tamagaki, Potential models of nuclear forces at small distances, Prog. Theor. Phys. **39**, 91 (1968).

[29] R. Tamagaki, Superfluid state in neutron star matter. I. Generalized Bogoliubov transformation and existence of $^3P_2$ gap at high density, Prog. Theor. Phys. **44**, 905 (1970).

[30] M. Hoffberg, A. E. Glassgold, R. W. Richardson, and M. Ruderman, Anisotropic superfluidity in neutron star matter, Phys. Rev. Lett. **24**, 775 (1970).

[31] M. Bender, P.-H. Heenen, and P.-G. Reinhard, Self-consistent mean-field models for nuclear structure, Rev. Mod. Phys. **75**, 121 (2003).

[32] S. Gandolfi, G. Palkanoglou, J. Carlson, A. Gezerlis, and K. E. Schmidt, The $^1S_0$ pairing gap in neutron matter, Condens. Matter **7**, 19 (2022).

[33] H. Sagawa, C. L. Bai, and G. Colò, Isovector spin-singlet ($T = 1, S = 0$) and isoscalar spin-triplet ($T = 0, S = 1$) pairing interactions and spin-isospin response, Phys. Scr. **91**, 083011 (2016).

[34] T. Oishi and N. Paar, Magnetic dipole excitation and its sum rule in nuclei with two valence nucleons, Phys. Rev. C **100**, 024308 (2019).

[35] T. Oishi, G. Kružić, and N. Paar, Discerning nuclear pairing properties from magnetic dipole excitation, Eur. Phys. J. A **57**, 180 (2021).

[36] D. Vautherin and D. M. Brink, Hartree-Fock calculations with Skyrme's interaction. I. Spherical nuclei, Phys. Rev. C **5**, 626 (1972).

[37] E. Perlińska, S. G. Rohoziński, J. Dobaczewski, and W. Nazarewicz, Local density approximation for proton-neutron pairing correlations: Formalism, Phys. Rev. C **69**, 014316 (2004).

[38] K. Bennaceur, A. Idini, J. Dobaczewski, P. Dobaczewski, M. Kortelainen, and F. Raimondi, Nonlocal energy density functionals for pairing and beyond-mean-field calculations, J. Phys. G: Nucl. Part. Phys. **44**, 045106 (2017).

[39] J. Dobaczewski, H. Flocard, and J. Treiner, Hartree–Fock–Bogolyubov description of nuclei near the neutron-drip line, Nucl. Phys. A **422**, 103 (1984).

[40] R. W. Richardson, Ginzburg-Landau theory of anisotropic superfluid neutron-star matter, Phys. Rev. D **5**, 1883 (1972).

[41] Y. Masaki, T. Mizushima, and M. Nitta, Microscopic description of axisymmetric vortices in $^3P_2$ superfluids, Phys. Rev. Res. **2**, 013193 (2020).

[42] M. Bender, K. Bennaceur, T. Duguet, P.-H. Heenen, T. Lesinski, and J. Meyer, Tensor part of the Skyrme energy density functional. II. Deformation properties of magic and semi-magic nuclei, Phys. Rev. C **80**, 064302 (2009).

[43] M. Bender, K. Rutz, P.-G. Reinhard, and J. A. Maruhn, Pairing gaps from nuclear mean-field models, Eur. Phys. J. A **8**, 59 (2000).

[44] N. Hinohara, Extending pairing energy density functional using pairing rotational moments of inertia, J. Phys. G: Nucl. Part. Phys. **45**, 024004 (2018).

[45] S. G. Rohoziński, J. Dobaczewski, and W. Nazarewicz, Self-consistent symmetries in the proton-neutron Hartree-Fock-Bogoliubov approach, Phys. Rev. C **81**, 014313 (2010).

[46] K. Bennaceur and J. Dobaczewski, Coordinate-space solution of the Skyrme-Hartree–Fock–Bogolyubov equations within spherical symmetry. The program HFBRAD (v1.00), Comput. Phys. Commun. **168**, 96 (2005).

[47] T. Yamaguchi and Y. Ohashi, Proposed method to realize the *p*-wave superfluid state using an *s*-wave superfluid Fermi gas with a synthetic spin-orbit interaction, Phys. Rev. A **92**, 013615 (2015).

[48] M. Beiner, H. Flocard, N. V. Giai, and P. Quentin, Nuclear ground-state properties and self-consistent calculations with the Skyrme interaction: (I). Spherical description, Nucl. Phys. A **238**, 29 (1975).

[49] E. Chabanat, P. Bonche, P. Haensel, J. Meyer, and R. Schaeffer, A Skyrme parametrization from subnuclear to neutron star densities. Part II. Nuclei far from stabilities, Nucl. Phys. A **635**, 231 (1998).

[50] G. Colò, H. Sagawa, S. Fracasso, and P. F. Bortignon, Spin–orbit splitting and the tensor component of the Skyrme interaction, Phys. Lett. B **646**, 227 (2007).

[51] T. Lesinski, M. Bender, K. Bennaceur, T. Duguet, and J. Meyer, Tensor part of the Skyrme energy density functional: Spherical nuclei, Phys. Rev. C **76**, 014312 (2007).

[52] Y. Kanada-En'yo and F. Kobayashi, Mixing of parity of a nucleon pair at the nuclear surface due to the spin-orbit potential in ^{18}F, Phys. Rev. C **90**, 054332 (2014).

[53] N. Hinohara and W. Nazarewicz, Pairing Nambu-Goldstone modes within nuclear density functional theory, Phys. Rev. Lett. **116**, 152502 (2016).